

Available online at www.scholarsresearchlibrary.com



Scholars Research Library
Der Pharmacia Lettre, 2022, 14 (4): 01-07
(<http://scholarsresearchlibrary.com/archive.html>)



FEM Investigation of Silver Nanospheres, Nanoellipsoid, Nanorods and Core Shell Structures for Hyperthermia

Muhammad Usama Daud*

Department of Physics, University of Riphah, Faisalabad, Pakistan

*Corresponding author: Muhammad Usama Daud, Department of Physics, University of Riphah, Faisalabad, Pakistan, E-mail: usamadaud@gmail.com

Received: 31-Mar-2022, Manuscript No. DPL-22-59113; Editor assigned: 04-Apr-2022, PreQC No. DPL-22- 59113 (PQ); Reviewed: 18-Apr-2022, QC No. DPL-22-59113; Revised: 25-Apr-2022, Manuscript No. DPL-22-59113 (R); Published: 2-May-2022, DOI: 10.37532/dpl.2022.14.1

ABSTRACT

The finite element analysis approach was utilized to examine the appropriateness of silver nano-rods, spheres, ellipsoids, and core-shell structures for cancer hyperthermia therapy. To eliminate the malignant cells, the temperature of the silver nanostructures was increased from 42 to 46°C. The time it took the nanostructures to reach this temperature when heated by an external source was also calculated. For the finite element study of hyperthermia based on silver nanostructures, the heat transport module in COMSOL multiphysics was employed. The heat sensitivity of various forms of silver nanostructures was studied by inserting them inside the tumor tissue's spherical domain. At various time intervals, the suggested geometries were heated. In order to attain the optimal treatment temperature, the geometries were optimized. When compared to alternative forms, silver nano-rods reach the correct temperature rapidly. Among all the investigated geometries, the silver nano-rods reached the greatest temperature of 44.3°C. Furthermore, the silver nano-ellipsoids had the largest core volume, which was utilized to determine thermal responsiveness. After 0.5 μ s of heating, thermal equilibrium was achieved in the treatment zone, making these structures appropriate for hyperthermia therapy.

Keywords: COMSOL multiphysics, Hyperthermia, Core-shell structure, Finite element analysis.

INTRODUCTION

Cancer is a disease in which a cell group develops uncontrolled. Cancerous cells do not respond to signals that trigger the normal cell cycle because their self-sufficiency is unchecked, resulting in uncontrolled cell growth and proliferation [1]. Because heat-stressed cells are more receptive to treatment, hyperthermia therapies are widely utilized in conjunction with other cancer treatments such as chemotherapy or

radiation therapy [2,3]. This kind of therapy employs external physical means to raise the temperature of the tumor site to between 42 and 46°C. A temperature rise might be localized or systemic, impacting the entire body and its treatment plan. Local hyperthermia, regional hyperthermia, and whole-body hyperthermia are the three kinds of hyperthermia. Local Hyper Thermia (LHT) has less adverse effects than chemo- and radiation therapy, and it may be used in combination with any standard therapeutic strategy [4]. There are three primary clinical techniques of high-temperature applications, which are controlled by the organ to target the tumor's stage. Localized, advancing or deep-seated, and disseminated malignancies are treated with localized, regional, and whole-body HT, respectively. Local HT is reserved for tiny tumors (≤ 3 cm to 5-6 cm in diameter) situated superficially or inside an accessible body cavity, such as the rectum or esophagus [5]. Whole-body hyperthermia is caused by heating the body with an external heat source, such as microwaves or radio frequencies, which might have negative side effects due to non-selective heating *via* a non-selective mechanism [6]. Regional hyperthermia is the heating of a large region of cells, such as a bodily cavity, limb, or organ. Regional hyperthermia can be achieved *via* the regional perfusion approach, often known as the Continuous Hyperthermia Peritoneal Perfusion (CHPP) strategy. The regional perfusion strategy involves drawing blood from the patient, heating it, and then pumping it back into the injured organ. The CHPP procedure is used to treat peritoneal malignancies, such as primary peritoneal mesothelioma and stomach cancer [7]. Cancer cells are eliminated in tiny places by injecting heat carriers (Fe, Co, Ni, Ag, Au, etc.) into the body. This is known as local body hyperthermia, and nanoparticles are utilized as heat sensors [8].

High-intensity focused ultrasounds, magnetic hyperthermia, microwave/radio frequencies, and plasmonic photo-thermal treatment can all be used to heat Nano Particles (NPs). The heating technique is chosen based on the specified conditions. Because all hyperthermia therapy methods have downsides, there is a need to find novel cancer treatment approaches that are more successful while also being less hazardous to healthy cells. The biocompatibility and functionalization of surface coating materials, as well as the selection of an appropriate core, are critical issues in the design of NPs for practical usage. Surface coatings can be made of noble metals, long-chain organic ligands, inorganic polymers, or organic polymers. Such coatings are important because they are utilized to bind functional groups such as biomarkers, peptides, and antibodies. These coatings are also employed to inhibit NP clustering caused by particle interactions, resulting in the stability of NP-prepared colloidal solutions. Furthermore, these coatings improve NP biocompatibility by preventing harmful ions from the magnetic core from leaching into the biological system [9,10].

Because of their distinctive physical and chemical properties, silver nanoparticles stand out among metallic nanomaterial for their applications in health-care goods, textiles, consumer items, medical devices, and bio sensing. AgNPs have excellent thermal, optical, and electrical characteristics, as well as antifungal, antibacterial, and antiviral activities [11-13]. AgNPs have recently aroused the interest of Nano medicine researchers, as many studies have demonstrated that these NPs can create antitumor effects in *in vitro* and *in vivo* tumor models, possibly benefitting a number of oncotherapy modalities and diagnostic tools [14-17]. In addition to antibacterial capabilities, AgNPs exhibit distinct lethal effects on mammalian cells, making silver-based nanoparticles potentially effective in tumor therapy. AgNPs therapeutic effectiveness is based on their specific mechanism of causing cell death in mammals. The reported work included a comparative analysis of heat generation utilizing a single silver nanoparticle, nano-sphere, nano-rod, and nano-ellipsoid. The volume of these forms is defined as follows: $V_{\text{ellipsoid}} = V_{\text{sphere}} = V_{\text{rod}}$. This model describes the thermal effect of heat propagation in the tumor cell, as well as the spatial-temporal distributions of temperature during therapy. Furthermore, the impact of various coating materials, such as gold (Au) and polymer (PEG), is investigated. The thickness of the shell is determined to be an important component that determines the thermal response of the treatment system *via* the thermal properties of the materials used. Finally, various amounts of NPs are connected to the core surface to imitate a partially coated coating surface. COMSOL Multiphysics' heat transfer module is employed to simulate the heating process of the nanostructures using finite element simulations [18].

MATERIALS AND METHODS

In this study, a single nanoparticle inside a radius of 500 nm with a spherical domain of tissue was investigated for different forms, as shown

in Figure 1. The primary purpose was to investigate the temperature response of biological tissue when a nanoparticle with a complicated core-shell structure and different shapes was used as a heating source (sphere, ellipsoid, and rod). The solution of the Fourier heat transfer equation provides the temperature distribution $T(x, y, z, \text{ and } t)$ in the tumor cell.

$$\rho C_p \frac{\partial T}{\partial t} + \nabla(-k\nabla T) = Q$$

Where ρ is the cell density, C_p is the specific heat capacity at constant pressure, k is the thermal conductivity of the cell, and the heat dissipated by nanoparticles in the cell volume is denoted by Q . The volumetric power density is constant, and its value is $Q=1016 \text{ (W m}^3\text{)}$ [19]. To study the heating process, the initial temperature of the tissue was kept $T_i 37^\circ\text{C}$, which is the normal temperature of the human body (Figure 1).

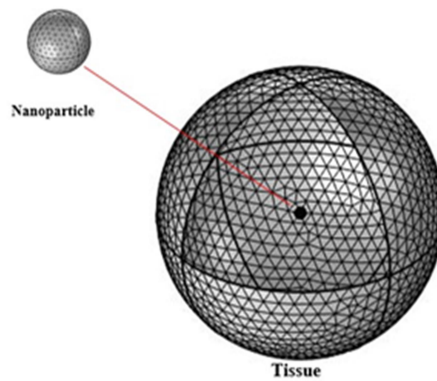


Figure 1: The geometry discretization.

Figure 2 depicts the analysis of silver nanostructures of various forms (sphere, rod, and ellipsoid). To begin, the spherical form of silver with a radius of 20 nm was investigated. By determining the dimensions for the rod and ellipsoid, the volume of the particle was kept the same as the other forms. The length of the cylinder for the Nano rod was $L_{cyl}=73 \text{ nm}$, the radius for the hemispherical caps $R_{cyl}=R_{cap}=11 \text{ nm}$, and the dimensions for the ellipsoid were 12-15-44.3 nm. The thickness of the Au and PEG polymer coating was chosen at 5, 10, 20, 30, and 40 nm to evaluate the coating effect (Figure 2).

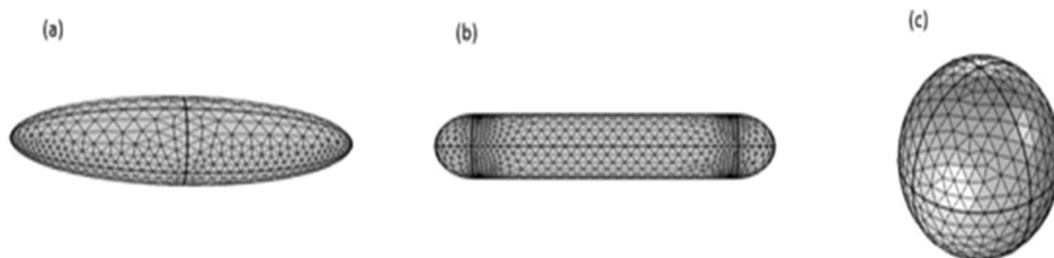


Figure 2: Different shapes used in simulations (a) Ellipsoid, (b) Rod, (c) Sphere.

For the aim of assessing the thermal development of the suggested structure, a core-shell structure with a radius of 20 nm was chosen. To compare the thermal reactions of the ellipsoidal and spherical surface coatings, three distinct coating surfaces (one spherical and two ellipsoidal) were simulated on the silver nanoparticle core. A gold coating was applied to a silver nanoparticle with a radius of 20 nm. Figure 3 depicts the simulated development of gold nanoparticles on the core of AgNP. Table 1 shows the thermal characteristics of the various materials employed in this investigation (Figure 3) (Table 1).

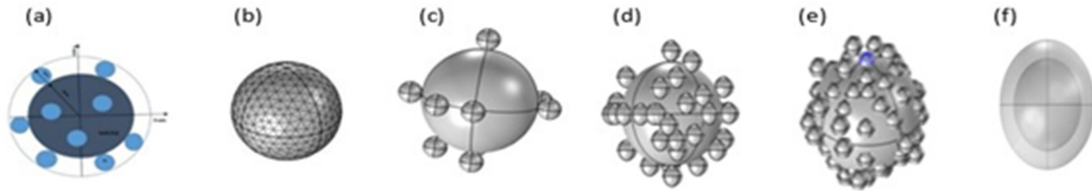


Figure 3: Shell structure (incomplete) Simulated in COMSOL Multiphysics (a) Naked core of radius 20 nm, AgNPs of 4 nm radius attached to core surface. (b) Core (c), (d), (e) 10, 40 and 70 nanoparticles attached to core, (f) Complete shell.

	Thermal conductivity [W/m ⁻¹ k]	Mass Density [kg/m ³]	Specific heat capacity [J/kg W/m ⁻¹ K]
Tissue [20]	0.512	1000	3800
Gold [21]	317	19300	129
Silver [22]	429	10500	235
Polymer [21]	0.2	1000	1000

Table 1: Thermal response of source materials used in the reported simulation work.

RESULTS AND DISCUSSION

To examine the possible use of silver nanoparticles (AgNPs) in hyperthermia, several geometries such as nano-rod, nano-ellipsoid, and nano-sphere were inserted in a spherical shape of tumor with a radius of 500 nm. The first simulation depicts the maximum temperature attained by the aforementioned geometries when heated by an external source in the tissue. As seen in figure 4, heating the nanoparticles thermal equilibrium of the tumoral cell over time (Figure 4).

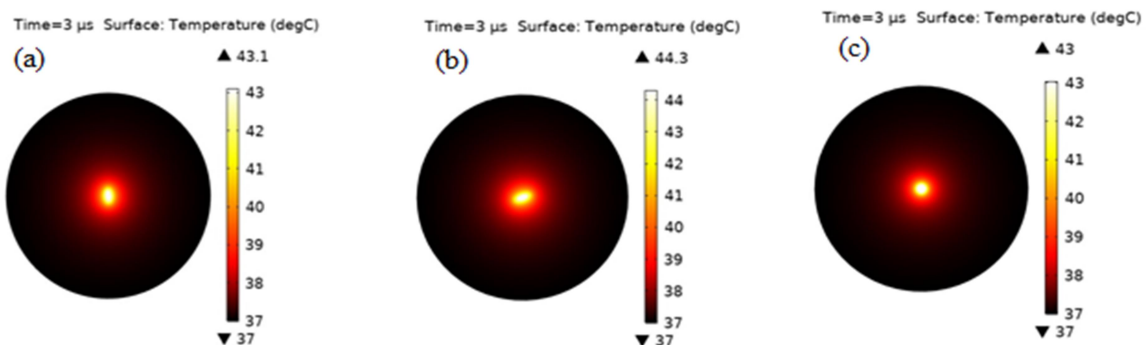


Figure 4: The 2 D spatial temperature distribution for from the beginning of heating process of 0.5 μ m tumoral cells by (a) Ellipsoid, (b) Rod, and (c) Sphere.

The temperatures attained by simulated forms differed, as seen in Figure 6. Given that the thermal response is dictated by heat generation by volume and surface, the temperature variance may be explained by a change in the proportional surface of each shape. $T_{max}=43^{\circ}\text{C}$ for the sphere, $T_{max}=43.1^{\circ}\text{C}$ for the ellipse, and $T_{max}=44.3^{\circ}\text{C}$ for the rod. As seen in Figure 5, these values are obtained from the core of the particles, which subsequently spread into the surrounding media. An ellipse has a larger thermal field spread than a sphere or a rod. In hyperthermia applications, NPs covered with different materials offer a useful surface. Simulations were used to explore the effect of the coating surface on heat dissipation in the surrounding medium. A silver (Ag) magnetic core with a gold or polymer-like shell was used as a heat source. The thermal conductivity co-efficient of the two simulated shell materials resulted in opposing heat dissipation effects as shell thickness increased. The thermal conductivity of gold dropped while that of polymer increased (Figure 5).

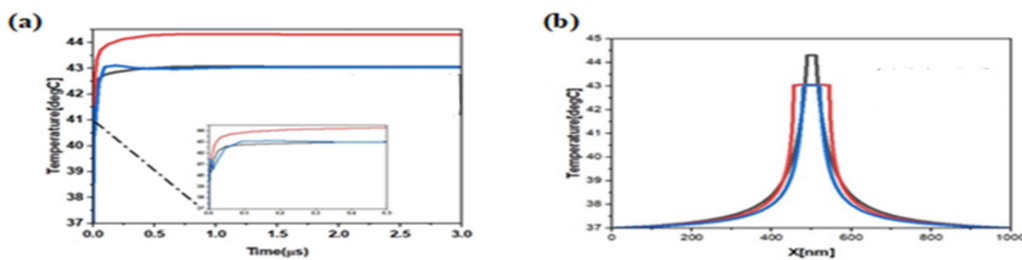


Figure 5: The time dependent and radial temporal distribution for three different shapes (a) Temperature evolution at the center of tumor ($x=0$) and (b) The radial distribution after 3 microseconds of heating process.

Note: (a) — Sphere, — Rod, — Ellipsoid (b) — Rod, — Ellipsoid, — Sphere

The hyperthermia process is linked to the functioning of core-shell structures. To achieve maximum temperature, a sphere with a radius of 20 nm was used for as-synthesized NP. The core of AgNPs was covered by a shell of Gold (Au) or PEG polymer in this sort of simulation, and the induced temperature by the core was examined. Different shell thicknesses were investigated, and the influence of temperature on the induced core of NPs is shown in figure 6. Temperature decreases with increasing thickness of Au shell and rises with increasing thickness of PEG polymer shell, as seen in the graph. Because gold (Au) has a high thermal conductivity, it quickly transmits heat to its surroundings. Polymers with limited thermal conductivity retain more heat within the particle, resulting in a temperature increase. Heat has a direct effect and influence on the conductivity value. These results in Figure 8 clearly demonstrate the possibility of adjusting temperature by varying the thickness of the shell. In addition, the temperature necessary for hyperthermia is regulated by material and shell thickness, which is dependent on the specific location of application in the human body (Figures 6 and 7).

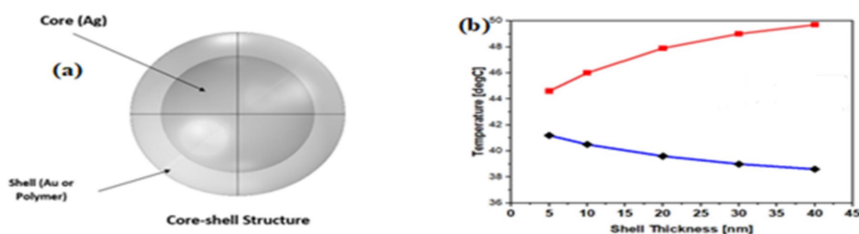


Figure 6: (a) The Core-shell structure. (b) The maximum temperature obtained by coating of Au (Gold) and PEG Polymer shells of thickness 5,10,20,30 and 40 nm.

Note: (b) Gold (Au) —◆— , Polymer —■—

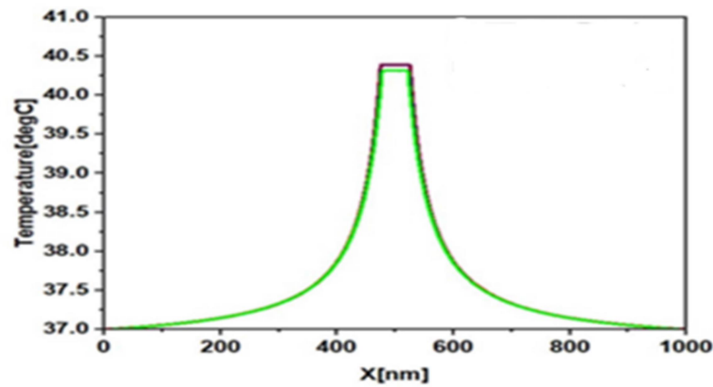


Figure 7: Radial temperature distributions of coating different shapes (1) Sphere of radius 20 nm, (2) Ellipsoid 1:25-25-43.2 nm, (3) Ellipsoid 2:22-25-49 nm.

Note: — Ellipsoid 1, — Sphere, — Ellipsoid 2

It is obvious from Figure 7 that there is no significant change in temperature of coating surfaces, indicating that anisotropy of coating surfaces is not crucial for the hyperthermia process. Because gold nanoparticles (AuNPs) have special qualities, they develop and create isolated islands, which then turn into an incomplete uneven coating, which finally transforms into a full shell enveloping the core. Small AuNPs with a radius of 4 nm were connected to the core surface of AgNPs with a radius of 20 nm, which were subsequently implanted in tissue with a radius of 500 nm. As shown in Figure 8, the volume-coverage ratio (percent) of AuNPs relative to the volume of the whole shell was calculated to explain the temperature profile for incompletely covered NPs with varied numbers of NPs attached. The highest temperature at the center of the NP was 42.3°C for naked core, with a progressive reduction in temperature as the quantity of surface coating increased, and the minimum temperature was 39.9°C at the center of the NP when a full shell developed (Figure 8).

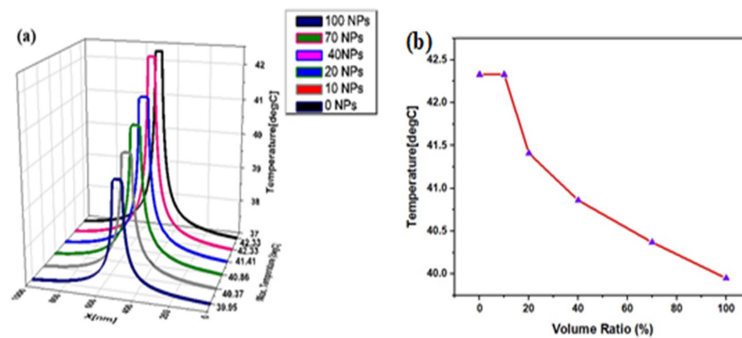


Figure 8: (a) Radial distribution of temperature after 3 μs of heating process for different levels of surface coating and (b) Temperature evolution for different volume coverage ratios.

CONCLUSION

Silver nanoparticles were chosen in this study because they are non-toxic, antiviral, and antibacterial, which are crucial for hyperthermia applications. In simulations, various forms such as spheres, rods, and ellipsoids were employed, and the simulations were conducted for 3 μs. When compared to other forms, the temperature obtained by silver nano-rod is the highest (i.e., T max=44.3°C). Size and form are critical for NP's therapeutic advantages. This finding can be used to improve the thermal performance of biomedical applications. The specific

thermal field absorption rate for different forms of NPs with the same volume was investigated. It was discovered that the silver nano-ellipsoid covered a bigger center volume than other forms due to its higher thermal absorption rate, with thermal equilibrium attained after 0.5 μ s from the start of the heating process. The effect of thickness and form on thermal increment or decrement was investigated, and it was discovered that the thermal characteristics of the shell define thermal increment or decrement. The maximum temperature attained by the noble metal core is enabled by shell thickness, although it is still modest. The simulation examined the heat response of the incomplete surface coating impact of varied gold shell covering volume ratios. Temperature evolution is discovered to alter the open surface left by the shell formation process. The utilization of core-shell NPs, which are composed of a noble metal core and a surrounding biocompatible surface, is based on the choice of acceptable materials, surface homogeneity, and surface coating thickness.

REFERENCES

- [1] Singh M. *J App Phy*, **2016**.
- [2] Sharma S K., Shrivastava N., Rossi F., et al., *Nano Today*, **2019**, 29:100795.
- [3] Jha S., Sharma P K., Malviya R. *Achiev Life Sci*, **2016**, 10(2):161-167.
- [4] Baronzio G., Parmar G., Ballerini M., et al., *J Integr Oncol*. **2014**, 3(115):2.
- [5] Wust P., Hildebrandt B., Sreenivasa G., et al., *Lancet Oncol*, **2002**, 3(8):487-497.
- [6] Habash RW., Bansal R., Krewski D., et al., *Crit Rev Biomed Eng*, **2006**, 34(6).
- [7] Falk M H., Issels R D. *Intern J Hyperthermia*, **2001**, 17(1):1-8.
- [8] Feldman A L., Libutti S K., Pingpank J F., et al., *J Clin Oncol*, **2003**, 21(24):4560-4567.
- [9] Roizin-Towle L., Pirro J P. *Int J Radiat Oncol Biol Phys*, **1991**, 20(4):751-756.
- [10] Fiorani D., Dormann J L., Cherkaoui R., et al., *J Magn Magn Mater*, **1999**, 196:143-147.
- [11] Lara H H., Garza-Treviño E N., Ixtepan-Turrent L., et al., *J Nanobiotechnol*, **2011**, 9(1):1-8.
- [12] Lu L., Sun R W., Chen R., et al., *Antivir Ther*, **2008**, 13(2):253-62.
- [13] Alshehri A H., Jakubowska M., Młodziński A., et al., *ACS Appl Mater Interfaces*, **2012**, 4(12):7007-7010.
- [14] Sánchez-López E., Gomes D., Esteruelas G., et al., *Nanomaterials*, **2020**,10(2):292.
- [15] Cameron S J., Hosseinian F., Willmore W G. *Int J Mol Sci*, **2018**, 19(7):2030.
- [16] Cosmol A. *J App Phy*, **2008**.
- [17] Taloub S., Hobar F., Astefanoaei I., et al., *Nanosci Nanotech*, **2016**, 6(1):55-61.
- [18] Saw C B., Loper A., Komanduri K., et al., *Med Dosimetry*, 2005, 30(3):145-148.
- [19] Govorov A O., Zhang W., Skeini T., et al., *Nanoscale Res Lett*, **2006**, 1(1):84-90.
- [20] Tippa S., Narahari M., Pendyala R. *AIP Conf Proc*, **2016**, 1787 (1):020014.
- [21] Hervault A., Thanh N T. *Nanoscale*, **2014**, 6(20):11553-11573.